Bioorg. Med. Chem. Lett. 41 (2021) 127996

Contents lists available at ScienceDirect

Bioorganic & Medicinal Chemistry Letters

journal homepage: www.elsevier.com/locate/bmcl

Structure–activity relationship studies of 3-substituted pyrazoles as novel allosteric inhibitors of MALT1 protease

Ken Nunettsu Asaba *, Yohei Adachi, Kazuyuki Tokumaru *, Akira Watanabe, Yasufumi Goto, Takumi Aoki

Pharmaceutical Research Laboratories, Toray Industries, Inc., 6-10-1 Tebiro, Kamakura, Kanagawa 248-8555, Japan

ARTICLE INFO

Keywords:
MALT1
Paracaspase
Allosteric inhibitors
Structure activity relationship

ABSTRACT

We report the discovery of a novel series of 1,5-bisphenylpyrazoles as potent MALT1 inhibitors. Structure–activity relationship exploration of a hit compound led to a potent MALT1 inhibitor. Compound **33** showed strong activity against MALT1 (IC_{50}: 0.49 μM), potent cellular activity (NF-κB inhibition and inhibition of IL2 production), and high selectivity against caspase-3, -8, and -9. The results of a kinetics study suggest that compound **33** is a non-competitive inhibitor of MALT1 protein.

The nuclear factor-κB (NF-κB) family of transcription factors is considered to play a central role in the immune systems, including immune-cell development, homeostasis, survival, and function.[1–4] NF-κB is implicated in the pathogenesis of several autoimmune diseases, such as rheumatoid arthritis, systemic lupus erythematosus, type I diabetes, multiple sclerosis, and inflammatory bowel disease.[5–11] Although NF-κB is activated transiently during the normal immune response, it is chronically activated in tissues affected by autoimmune diseases and induces excessive inflammatory cytokines and chemokines, which leads to autoimmunity.

Mucosa-associated lymphoid tissue lymphoma translocation protein 1 (MALT1) is related to the activation of NF-κB signaling and the negative feedback loop required for this signaling.[12–16] MALT1 acts as a scaffold protein, resulting in protein–protein interactions which lead to the activation of the IκB kinase complex and subsequent activation of NF-κB. In addition to this function, MALT1 is a protease. The paracaspase (cysteine protease) domain of MALT1 cleaves RelB, CYLD, and A20, all of which function as negative regulators of canonical NF-κB signaling. Therefore, MALT1 is an important therapeutic target for the treatment of immunomodulation disorders and lymphoma. In this study, we describe the discovery and structure–activity relationship (SAR) exploration of a series of allosteric small-molecule inhibitors of MALT1 protease.

Phenothiazine derivatives, including mepazine, thioridazine (**1**), and promazine, target the allosteric site of MALT1, preventing rearrangement of the protein from the inactive state to the activated state and inhibiting proteolytic cleavage of the substrate (Table 1).[17,18] None of these phenothiazine derivatives significantly inhibits either caspase 3 or caspase 8, which are structurally the closest relatives of MALT1 in mammals.

We conducted molecular docking simulations with MALT1 to identify selective small inhibitors of MALT1. The model was constructed from the crystal structure of MALT1 complexed with the allosteric inhibitor thioridazine (PDB ID: 4I1R), and we used thioridazine (**1**) as the template compound for docking. Enzymatic biochemical assay of the top ranked compounds identified compound **2**, which showed weak activity against MALT1 (Table 1). The calculated docking pose of **2** indicated that the 1,5-bisphenylpyrazole moiety is located similarly to the

Table 1
In vitro activity profiles of thioridazine (**1**) and compound **2.**

Thioridazine (**1**)	**2**
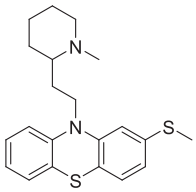	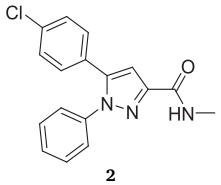
MALT1 IC_{50}: 3.43 μM	MALT1 IC_{50}: 19.79 μM

* Corresponding author.
E-mail addresses: kennunettsu.asaba.u8@mail.toray (K.N. Asaba), kazuyuki.tokumaru.n6@mail.toray (K. Tokumaru).

https://doi.org/10.1016/j.bmcl.2021.127996
Received 18 January 2021; Received in revised form 15 March 2021; Accepted 20 March 2021
Available online 26 March 2021

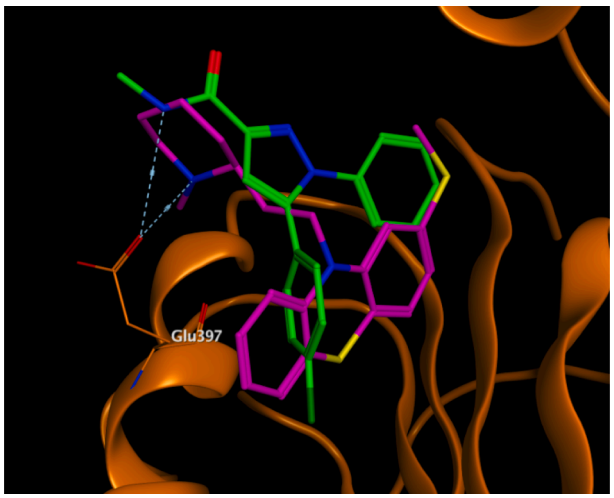

Fig. 1. Docking pose of compound **2** (green) in the crystal structure of MALT1 bound with thioridazine (**1**, purple) (PDB ID: 4I1R).

phenothiazine moiety of thioridazine (**1**) bound in the hydrophobic pocket of MALT1 (Fig. 1). The pose also showed that a hydrogen bond is formed between the *N*-methylamide nitrogen of **2** and glutamic acid E397, again similar to the crystal structure with thioridazine (**1**).[17] We selected this 3-substituted pyrazole compound as a starting point as it has three sites for initial structure–activity studies, namely, two phenyl rings and a substituted amide.

Scheme 1 illustrates the synthesis of 1,5-bissubstituted pyrazole-3-carboxamides (**V**). Commercially available ketones (**I**) were condensed with diethyl oxalate using sodium ethoxide in ethanol. The obtained ethyl 2,4-dioxobutanoates (**II**) were treated with hydrazines in ethanol to give ethyl 1*H*-pyrazole-3-carboxmides (**III**). Compounds **III** were hydrolyzed to 1*H*-pyrazole-3-carboxylic acids (**IV**) using aqueous sodium hydroxide solution in ethanol. Target compounds **V** were synthesized by the condensation of compounds **IV** with amines using amide coupling reagents such as carbonyldiimidazole and 1-[bis(dimethylamino)methylene]-1H-1,2,3-triazolo[4,5-*b*]pyridinium 3-oxide hexafluorophosphate (HATU).

Substituents at the 5-position can be introduced by different methods, as shown in Scheme 2. 1-(4-Chlorophenyl)-5-hydroxy-1*H*-pyrazole-3-carboxylic acid (**VIII**) was synthesized using 4-chlorophenylhydrazine hydrochloride and dimethyl acetylenedicarboxylate. Next, **VIII** was converted to 1-(4-chlorophenyl)-3-(methylcarbamoyl)-1H-pyrazol-5-yl trifluoromethanesulfonate ester (**X**) via amidation and sulfonylation; then, **X** was coupled with boronic acid derivatives to obtain 1,5-bissubstituted pyrazole-3-carboxamides (**V**).

We first introduced various substituents at the 1-position of 1*H*-

Table 2

SAR for the 1-position of 1*H*-pyrazoles.

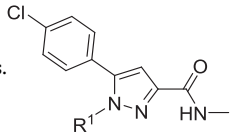

compound	R^1	MALT1 inhibition IC_{50} (μM)	MALT1 inhibition at 25 μM
2	Ph	19.79	59%inh
3	Benzyl	16.33	57%inh
4	Cyclohexyl	not tested	63%inh
5	Me	>25	7.7%inh
6	4-Chlorophenyl	7.01	72%inh
7	3-Chlorophenyl	not tested	57%inh
8	2-Chlorophenyl	>25	46%inh

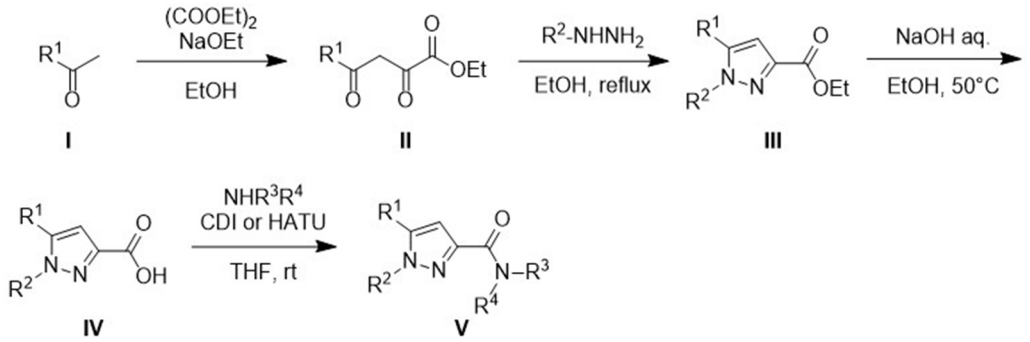

Scheme 1. Synthesis of compounds **V** via a condensation reaction at the last step.

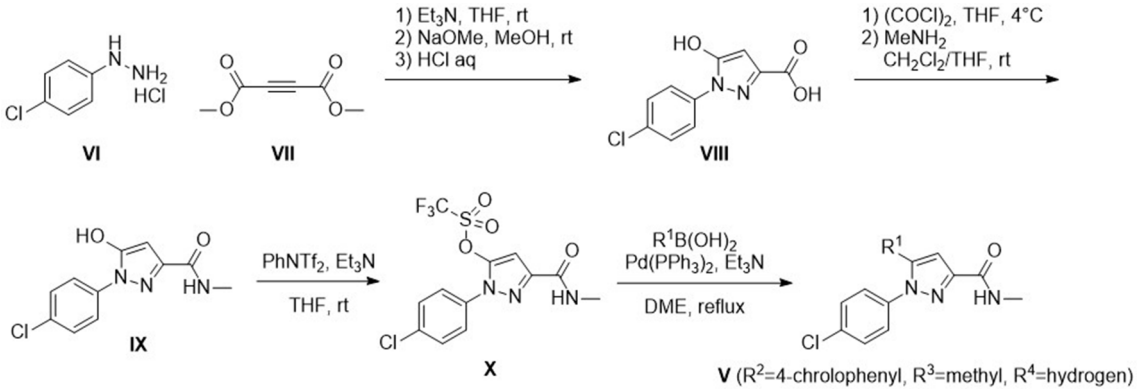

Scheme 2. Synthesis of compounds **V** via Suzuki coupling at the last step.

Table 3

SAR for the 5-position of 1*H*-pyrazoles.

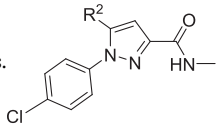

compound	R^2	MALT1 inhibition IC_{50} (μM)	MALT1 inhibitionat 25 μM
6	4-Chlorophenyl	7.01	72%inh
9	3-Chlorophenyl	>25	43%inh
10	2-Chlorophenyl	>25	23%inh
11	Ph	16.79	61%inh
12	4-Methoxyphenyl	6.55	80%inh
13	4-Fluorophenyl	>25	47%inh
14	4-Trifluoromethylphenyl	>25	47%inh
15	4-Hydroxymethylphenyl	>25	19%inh
16	4-Methanesulfonylphenyl	>25	5.7%inh
17	4-Trifluoromethoxyphenyl	>25	38%inh
18	4-Cyanophenyl	>25	31%inh
19	3-Thienyl	>25	26%inh
20	2-Furyl	>25	20%inh
21	3-Furyl	>25	16%inh
22	2-Methoxy-5-pyridyl	>25	21%inh

pyrazole (Table 2). The benzyl (**3**) and cyclohexyl (**4**) derivatives exhibited potency similar to that of compound **2**, whereas methyl derivative (**5**) was completely inactive, suggesting that large hydrophobic substituents such as phenyl groups are required to fill the hydrophobic pocket in MALT1. We performed chloride scanning to identify the optimal substitution position and identified 4-chlorophenyl (**6**) as the most potent of the chloride-substituted phenyls (**7**, **8**). Substituents at the 5-position of 1*H*-pyrazole were explored by fixing 4-chrolophenyl as the 1-position substituent, then introducing substituents at the 5-position to identify moieties more potent than phenyl (Table 3). In addition, we examined the effect of removing the chloride or changing the substitution position of the chloride, and found that both attenuated MALT1 inhibition (**9**, **10**, **11**). Other *p*-substituted phenyl groups were explored. The potency of the 4-methoxyphenyl (**12**) derivative was similar to that of **2**, whereas substitution with other *p*-substituted phenyl groups such as 4-fluorophenyl (**13**) or heteroaromatics such as 3-thienyl (**19**) provided inactive compounds. In particular, compounds with polar functional group substituents (**15**, **16**, **20**, **21**, **22**) had significantly less potency compared with **2**, consistent with the docking result (Fig. 1) showing the phenyl ring located to the hydrophobic pocket of MALT1.

Next, we explored substitutes at the 3-position (Table 4). Comparing secondary amide (**6**) to tertiary amides (**23**, **24**), amide hydrogen is essential for increased potency. This result was consistent with the binding mode of compound **2** shown in Fig. 1, which implies that the amide hydrogen of compound **6** interacts with E397. The potency of the aminoethyl (**25**) and hydroxyethyl (**27**) derivatives was similar to or higher than that of **6**, whereas the aminopropyl (**26**), hydroxypropyl (**28**), and aminocarbonylethyl (**29**) derivatives were less potent. The phenylethyl (**30**) and cyclohexylmethyl (**31**) were inactive. These results indicate that hydrophilic substituents such as amino and hydroxyl groups are favorable substituents at the 3-position. Therefore, we next focused on the amino groups. Introducing a methyl group into **25** provided more potent compounds (**32**, **33**), with *N*,*N*-dimethylaminoethyl (**33**) being 14-fold more potent than compound **6**. The acetoamide (**34**) and sulfonylamide (**35**) derivatives exhibited less potencies compared to **25** or **33**, showing that the basicity of the amine is a key factor to improving potency. Lengthening the carbon chain of compound **33** led to the slightly less potent compounds **36** and **37**, suggesting that optimal

Table 4

SAR for the 3-position of 1*H*-pyrazoles.

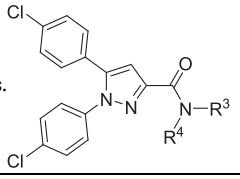

compound	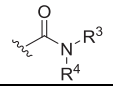	MALT1 inhibition IC_{50} (μM)
6	-CONHMe	7.01
23	-$CONMe_2$	21.18
24	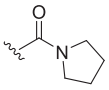	>25
25	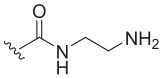	1.98
26	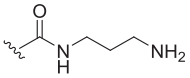	7.39
27	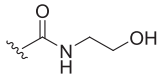	6.55
28	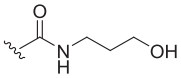	12.41
29	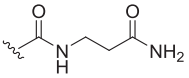	13.39
30	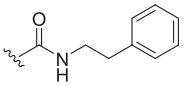	>25
31	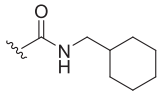	>25
32	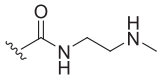	0.800
33	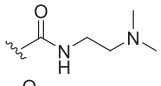	0.490
34	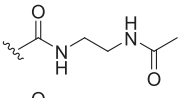	3.30
35	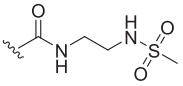	4.37
36	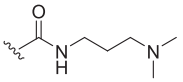	2.63
37	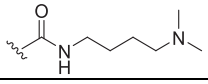	2.22

carbon chain length may be important for improving inhibitory activity. For example, in a series of 1,5-bisphenylpyrazoles, the ethylene linker is advantageous (**33** vs. **36** vs. **37**; **25** vs. **26**; **27** vs. **28**).

Cyclized substituents were introduced into *N*,*N*-dimethylaminoethyl (**33**) (Table 5). *N*,*N*-Dimethylaminopiperidine (**38**) had weak potency compared with **33** but was more potent than pyrrolidine (**24**) lacking an *N*,*N*-dimethylamino moiety. Inhibitory potency against MALT1 was enhanced by introducing amino groups at appropriate positions,

Table 5

Cyclized substituents

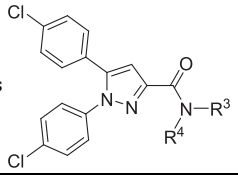

compound	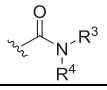	MALT1 inhibition IC_{50} (μM)
38	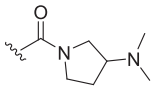	10.62
39	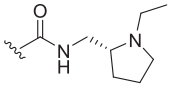	2.10
40	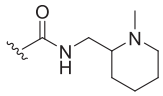	0.521
41	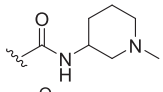	1.70
42	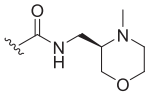	2.01
43	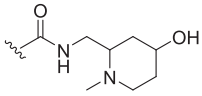	0.993
44	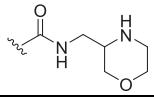	0.819

Table 6

Cellular activities of thioridazine (**1**) and compounds **6** and **33**.

Compounds	NF-κB inhibition IC_{50}	Inhibition of IL2 production IC_{50}
Thioridazine (**1**)	not tested (85%inh)	not tested (95%inh)
Compound **6**	9.34 μM (25%inh)	4.26 μM (54%inh)
Compound **33**	5.41 μM (82%inh)	1.79 μM (94%inh)

Numbers in parentheses represent the percent inhibition at 5 μM concentration.

suggesting that amino group interact with an amino acid of MALT1. The potency of the *N*-methylpiperidin-2-ylmethyl derivative (**40**) was similar to that of **33**, whereas other cyclized substituents resulted in decreased potency (**39**, **41**). Lipophilic efficiency (LipE) is an important metric for optimizing potency and ADME (absorption, distribution, metabolism, and excretion) properties.[19,20] To improve lipophilic efficiency, an oxygen atom was introduced into **40** to provide the 4-hydroxy-1-methylpiperidin-2-ylmethyl derivative (**43**) and removal of the methyl group from **42** to provide the morpholin-3-ylmethyl derivative (**44**). The LipE of **43** and **44** was improved compared to that of **33** and **6** (1.62, 1.50, 1.02, and 0.28 respectively).

The cellular activities of three compounds (thioridazine (**1**) and compounds **6** and **33**) were evaluated (Table 6). The inhibition of NF-κB activity and IL2 production by compound **33** (82%inh, 94%inh) was stronger than that of compound **6** (25%inh, 54%inh) and similar to that

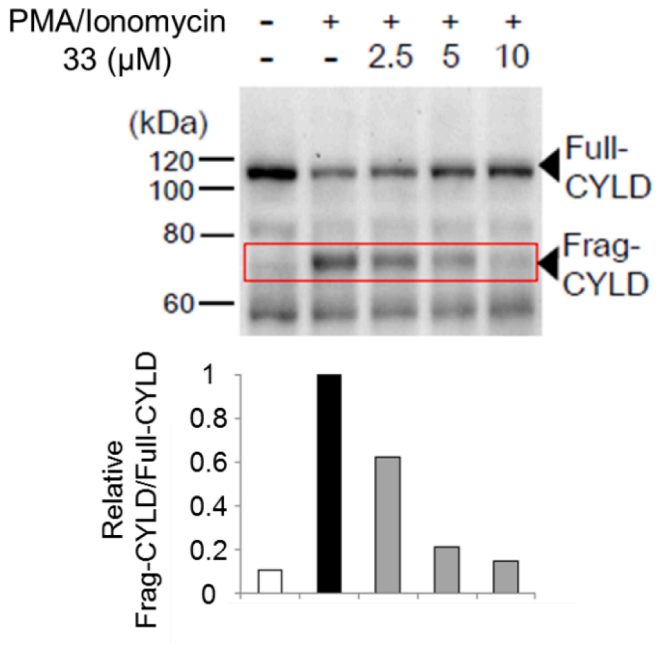

Fig. 2. Inhibition of MALT1-mediated CYLD cleavage by compound **33** by western blotting. Relative Frag-CYLD/Full-CYLD values are the value relative to the positive control (PMA/Ionomycin(+), 33(−)).

of thioridazine (**1**) (85%inh, 94%inh). Additionally, to confirm the direct inhibition of MALT1 substrate cleavage, degradation of CYLD in Jurkat cells was measured by western blotting (Fig. 2). Compound **33** dose-dependently decreased CYLD degradation product (Frag-CYLD) induced by PMA/Ionomycin stimulation. The value of relative Frag-CYLD/Full-CYLD ratio of **33** at 10 μM was same as that of unstimulated cells without MALT1 activation.

We investigated the selectivity of **33** against caspase-3, −8, and −9, which are structurally related to paracaspase, using a caspase drug screening kit (Promokine) according to the manufacturer's protocol (Fig. 3). The pan-caspase inhibitor Z-VAD-fmk was used as a positive control for each experiment. Compound **33** exhibited little activity against caspase-3, −8, and −9, even at concentrations up to 100 μM, showing it is a selective MALT1 paracaspase inhibitor.

A kinetics study was conducted to investigate the mode of action of **33** (Fig. 4). Compound **33** at a concentration around the IC_{50} (0.5 μM) strongly decreased Vmax, from 35,612 to 19,979 RFU/s, while Km remained essentially unchanged (246.9 to 234.2 μM), showing that compound **33** is a non-competitive inhibitor. This suggests that **33** does not bind to the paracaspase active site but rather to an allosteric pocket.

In summary, SAR exploration of hit compound **2** identified by screening led to the discovery of 1,5-bisphenylpyrazoles as novel, potent, and selective MALT1 inhibitors. Our exploration showed that phenyl rings are required to maintain potency, and the secondary amide with an aminoethyl moiety is an essential substructure for improved potency. Derivatization of the 3-position of 1*H*-pyrazoles led to compound **33**, which exhibits cellular activity similar to that of thioridazine (**1**). Investigation of the binding mode of **33** indicated a non-competitive inhibition mechanism against MALT1 protein. Further studies on structural optimization and identification of the binding site of this series of compounds is in progress.

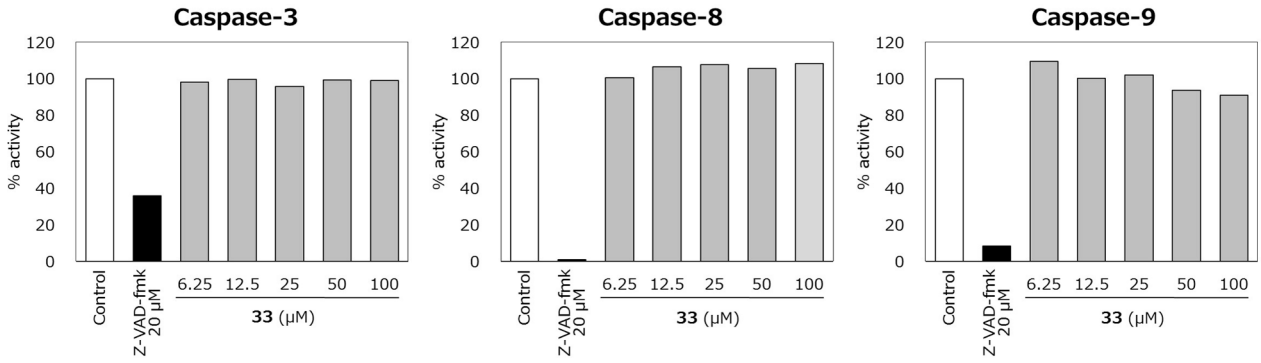

Fig. 3. Selectivity of compound **33** against caspase-3, -8, and -9.

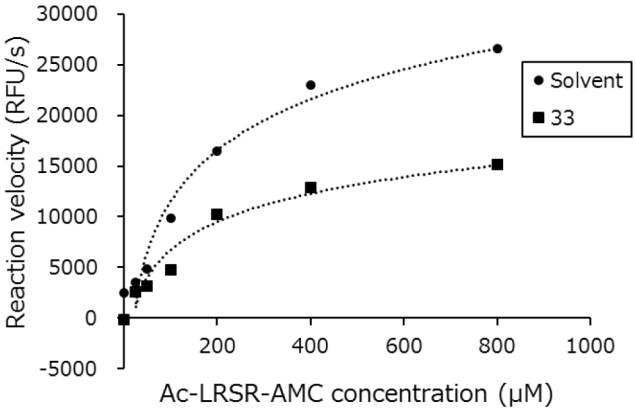

Substrate	Vmax (RFU/s)	Km (μM)
Solvent	35612	246.9
33	19979	234.2

Fig. 4. Michaelis-Menten kinetics (determined by increasing the concentration of the Ac-LRSR-AMC substrate in the absence or presence of 0.5 μM **33**).

Declaration of Competing Interest

The authors declare that they have no known competing financial interests or personal relationships that could have appeared to influence the work reported in this paper.

Appendix A. Supplementary data

Supplementary data to this article can be found online at https://doi.org/10.1016/j.bmcl.2021.127996.

References

1 DiDonato JA, Mercurio F, Karin M. *Immun Rev*. 2012;246:379–400.
2 Hayden Matthew S, Ghosh Sankar. *Cell Res*. 2011;21:223–244.
3 Hayde MS, West AP, Ghosh S. *Oncogene*. 2006;25:6758–6780.
4 Liang Yan, Zhou Yang, Shen Pingping. *Cell Mol Immunol*. 2004;1(5):343–350.
5 Sun S-C, Chang J-H, Jin J. *Trends Immunol*. 2013;34(6):282–289.
6 Herrington Felicity D, Carmody Ruaidhrí J, Goodyear Carl S. *J Biomol Screen*. 2016;21:223–242.
7 Pai S, Thomas R. *J Autoimmun*. 2008;31:245–251.
8 Greve B, Weissert R, Hamdi N, et al. *J Immunol*. 2007;179:179–185.
9 Han Z, Boyle DL, Manning AM, Firestein GS. *Autoimmunity*. 1998;28:197–208.
10 Isabelle Cleynen, Peter Jüni, GeertruidaBekkering E, et al. *PLoS One*. 2011;6(9), e24106.
11 Liu Ting, Zhang Lingyun, Joo Donghyun, et al. *Signal Transduct Target Ther*. 2017;2:17023.
12 Klein Theo, Fung Shan-Yu, Renner Florian, et al. *Nat Commun*. 2015;6:8777.
13 Rosebeck Shaun, Rehman Aasia O, Lucas Peter C, et al. *Cell Cycle*. 2011;10(15):2485–2496.
14 Afonina Inna S, Elton Lynn, Carpentier Isabelle, et al. *FEBS J*. 2015;282(17):3286–3297.
15 Coornaert Beatrice, Baens Mathijs, Heyninck Karen, et al. *Nat Immunol*. 2008;9:263–271.
16 Hailfinger Stephan, Nogai Hendrik, Pelzer Christiane, et al. *Proc Natl Acad Sci U S A*. 2011;108(35):14596–14601.
17 Schlauderer Florian, Lammens Katja, Nagel Daniel, et al. *Angew Chem Int Ed Engl*. 2013;52:10384–10387.
18 Nagel Daniel, Spranger Stefani, Vincendeau Michelle, et al. *Cancer Cell*. 2012;22:825–837.
19 Ryckmans Thomas, Edwards Martin P, Horne Val A, et al. *Bioorg Med Chem Lett*. 2009;19:4406–4409.
20 Johnson Ted W, Gallego Rebecca A, Edwards Martin P. *J Med Chem*. 2018;61:6401–6420.